SCIENTIFIC REPORTS

OPEN

On-chip optical mode exchange using tapered directional coupler

Zhonglai Zhang*, Xiao Hu* & Jian Wang

Received: 04 February 2015
Accepted: 06 October 2015
Published: 04 November 2015

We present an on-chip optical mode exchange between two multiplexed modes by using tapered directional couplers on silicon-on-insulator platform. The device consisting of mode multiplexing and mode exchange is compact with relatively large fabrication error tolerance. The simulation results show efficient higher order mode excitation and mode exchange. A low excess loss less than 0.5 dB and high extinction ratio larger than 15 dB over 10 nm wavelength range from 1535 to 1545 nm are achieved.

On-chip optical interconnect is a promising technique to satisfy the exponentially increasing demand of bandwidth for future massively-parallel chip multiprocessors[1]. Several techniques have been employed to extend the capacity of optical interconnections. Among them, wavelength-division multiplexing (WDM) is a straightforward way to expand the capacity with multiple wavelengths and has been widely used in long-haul optical communication systems. However, the requirement of multiple laser sources with different wavelengths could be expensive and complicated for on-chip optical interconnection applications. Space-division multiplexing (SDM), which only employs a single wavelength carrier, is another simple way and has been demonstrated by employing multi-core or few-mode fibers[2,3]. Mode-division multiplexing (MDM) is a kind of SDM technique which could provide an alternative approach to increasing the link capacity of optical interconnects. The key challenge of an on-chip MDM system is the efficient mode (de)multiplexer. Several kinds of (de)multiplexer have been proposed. The designs based on Y-junctions[4–7], multimode interferometer[8,9] and adiabatic couplers[10] mainly (de)multiplex two channels. In the recent years, schemes using asymmetrical directional couplers (ADC) have been proposed[11,12] and 8-channel hybrid (de)multiplexing combing MDM and polarization-division multiplexing (PDM) has been demonstrated[12]. The ADC can be easily fabricated on silicon-on-insulator (SOI) platform. In order to improve the fabrication tolerance of the ADC, a tapered coupling region is introduced into the ADC[13].

Very recently, on-chip MDM technology has attached increasing interest. Beyond basic functions such as (de)multiplexer, a laudable goal would be to develop data traffic grooming functions in on-chip MDM systems. Data traffic grooming is considered to be an attractive technique for enhancing the efficiency and flexibility of networks[14]. Lots of data traffic grooming functions have been well studied in WDM systems. Among these functions, data exchange, also known as wavelength exchange/interchange in the wavelength domain[15–20], is an important technique which can efficiently utilize network resources and facilitate superior network performance. In this scenario, one might also expect to implement data exchange in the mode domain in an on-chip MDM system, i.e. on-chip optical mode exchange[21].

In this paper, we present an optical exchange function in the mode domain based on tapered directional couplers on SOI platform. We calculate the mode properties of the SOI based nanowires and numerically study the light propagation for optical mode exchange by three dimensional finite difference time domain (3D FDTD) simulations.

Results

Structure of the tapered directional coupler. Figure 1 illustrates the structure of the tapered directional coupler, which couples light from a narrow silicon access waveguide (waveguide width w_1) to a tapered wide multimode bus waveguide (waveguide width from w_a to w_b with center width of w_2).

Wuhan National Laboratory for Optoelectronics, School of Optical and Electronic Information, Huazhong University of Science and Technology, Wuhan 430074, Hubei, China. *These authors contributed equally to this work. Correspondence and requests for materials should be addressed to J.W. (email: jwang@hust.edu.cn)

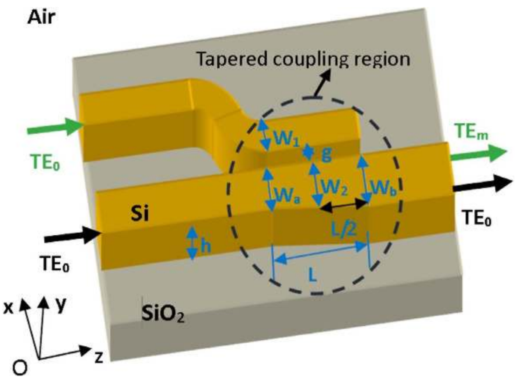

Figure 1. Schematic structure of a mode (de)multiplexer based on a tapered directional coupler.

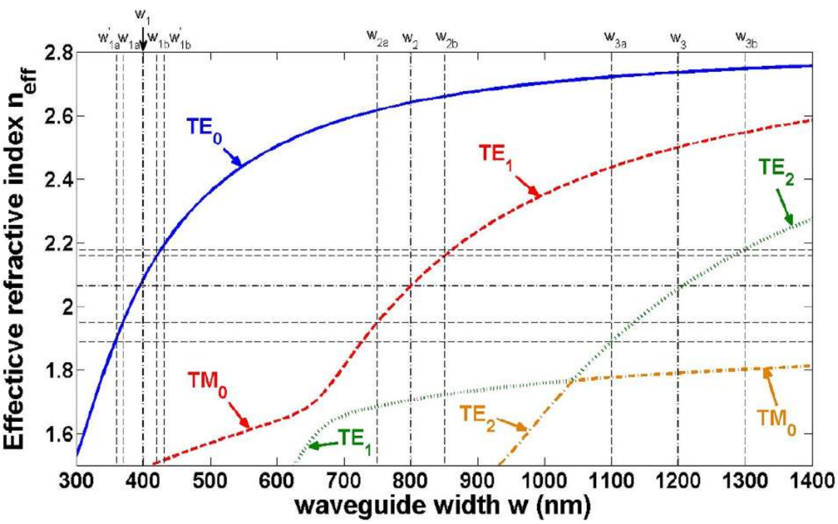

Figure 2. Effective indices of the TE_0, TE_1, TE_2 and TM_0 modes of an air-cladded SOI waveguide as a function of the waveguide width w for a waveguide height h = 220 nm.

The fundamental mode TE_0 in the access waveguide is coupled into the multimode bus waveguide through the tapered coupling region and converted to higher order mode TE_m (m = 1, 2, 3…). The coupling length is L and the gap between the two waveguide is g. When $w_a = w_b = w_2$, the structure is a conventional directional coupler, and high efficiency TE_0-TE_m coupling occurs when a phase matching condition ($n_{eff0} = n_{effm}$, where n_{eff0} is the effective index of the fundamental mode in the access waveguide and n_{effm} is the m^{th} higher order mode in the multimode bus waveguide) is satisfied. However, a large fabrication error of the access waveguide can easily break the phase matching condition in the conventional directional coupler.

Characterization of mode properties. Figure 2 shows the calculated effective refractive indices of the guided-modes in an SOI nanowire with different waveguide width. It can be seen that the slope of the effective refractive index of the TE_0 mode versus waveguide width is larger than other modes, so the fabrication error induced effective refractive index deviation of TE_0 mode is also larger than other modes, which means the phase matching condition is more easily to be broken. A tapered wide bus waveguide in the coupling region can relax the limitation. For the two widths w_{2a} (w_{3a}) and w_{2b} (w_{3b}) of the wide tapered waveguide, the corresponding widths of the narrow waveguide which satisfy the phase matching condition (n_{eff0} (w_1) = n_{effm} (w_m)) are w_{1a} (w_{1a}') and w_{1b} (w_{1b}'), respectively, as indicated in Fig. 2. Consequently, tapering the wide waveguide from w_{2a} (w_{3a}) to w_{2b} (w_{3b}) will result in a deviation tolerance between w_{1a} (w_{1a}') and w_{1b} (w_{1b}') for the narrow waveguide, within which a phase matching position can always be found along the taper. One thing should be noted is that w_{1a} (w_{1a}') should not be too close to the width where the TE_1 (TE_2) and TM_0 modes are hybridized (~660 nm for TE_1 and ~1040 nm for TE_2 in Fig. 2).

The mode distribution and effective refractive index of the TE_0, TE_1 and TE_2 modes in the silicon nanowire are displayed in Fig. 3(a–g). As shown in Fig. 3(c,f), the effective refractive index of TE_1 mode

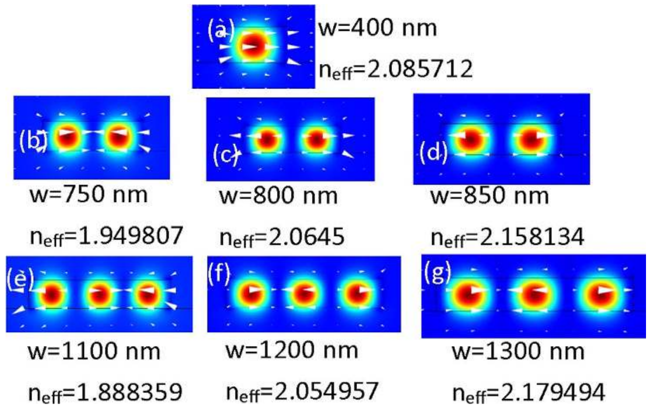

Figure 3. Mode distribution and effective refractive index of (**a**) TE_0 mode, (**b–d**) TE1 mode and (**e–g**) TE2 mode.

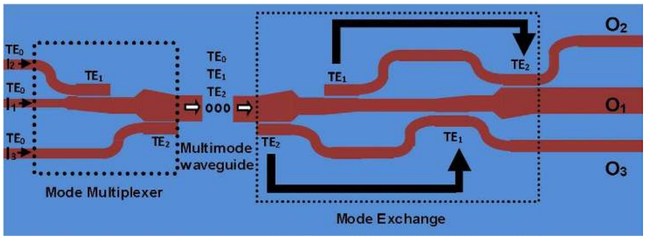

Figure 4. Schematic configuration of optical mode exchange.

with the waveguide width of 800 nm and the effective refractive index of TE_2 mode with the waveguide width of 1200 nm are nearly equal to the effective refractive index of TE_0 mode with the waveguide width of 400 nm, which means the phase matching condition can be satisfied.

Configuration of mode exchange. The proposed mode exchange configuration is depicted in Fig. 4. The left part in the dashed rectangle is a mode multiplexer. The TE_0 mode launched in the input port 1 (I_1) propagates directly in the wide multimode bus waveguide without any change. The TE_0 modes launched in the input port 2 (I_2) and input port 3 (I_3) are coupled into the multimode bus waveguide and converted into the high-order TE_1 mode and TE_2 mode by tapered directional couplers, respectively. The three multiplexed modes carrying different data information propagate through the wide multimode bus waveguide simultaneously. The right part in the dashed rectangle accomplishes the mode exchange function. On one hand, TE_2 mode is coupled into the lower narrow access waveguide as TE_0 mode and then coupled back into the multimode bus waveguide as TE_1 mode, i.e. mode conversion from TE_2 to TE_1 in the multimode bus waveguide. On the other hand, TE_1 mode is coupled into the upper narrow access waveguide as TE_0 mode and then coupled back into the multimode bus waveguide as TE_2 mode, i.e. mode conversion from TE_1 to TE_2 in the multimode bus waveguide. In this way, mode exchange function between the TE_1 mode and TE_2 mode can be realized. Meanwhile, the data information carried by the two modes is also exchanged. Mode coupling in the mode exchange part is also achieved by tapered directional couplers.

Mode exchange results. Figure 5 depicts the light propagation simulation results. Shown in Fig. 5(a) is the overall view of the light propagation with mode exchange. TE_0 mode is launched into both I_2 and I_3, leading to the simultaneous excitation of both TE_1 and TE_2 modes in the multimode bus waveguide. Shown in Fig. 5(b,c) are the zoomed in views of TE_1 mode excitation and TE_2 mode excitation by the launched TE_0 mode. In this way, both TE_1 mode and TE_2 mode exist and propagate in the multimode bus waveguide and mode multiplexing is achieved. The TE_1 (TE_2) mode is then coupled into an access waveguide (TE_0 mode) which is further coupled back into the multimode bus waveguide as the TE_2 (TE_1) mode. Shown in Fig. 5(d) is the zoomed in view of TE_2-TE_0-TE_1 mode conversion process. Shown in Fig. 5(e) is the zoomed in view of TE_1-TE_0-TE_2 mode conversion process. As a consequence, mode exchange between TE_1 and TE_2 modes ($TE_1 \leftrightarrow TE_2$) is implemented.

In order to clearly show the mode exchange process, we further simulate the light propagation with field monitors placed in the waveguide cross section when only one input port is launched by TE_0 mode. Figure 6(a) shows the case when only I_1 port is launched by TE_0 mode. It can be seen that the

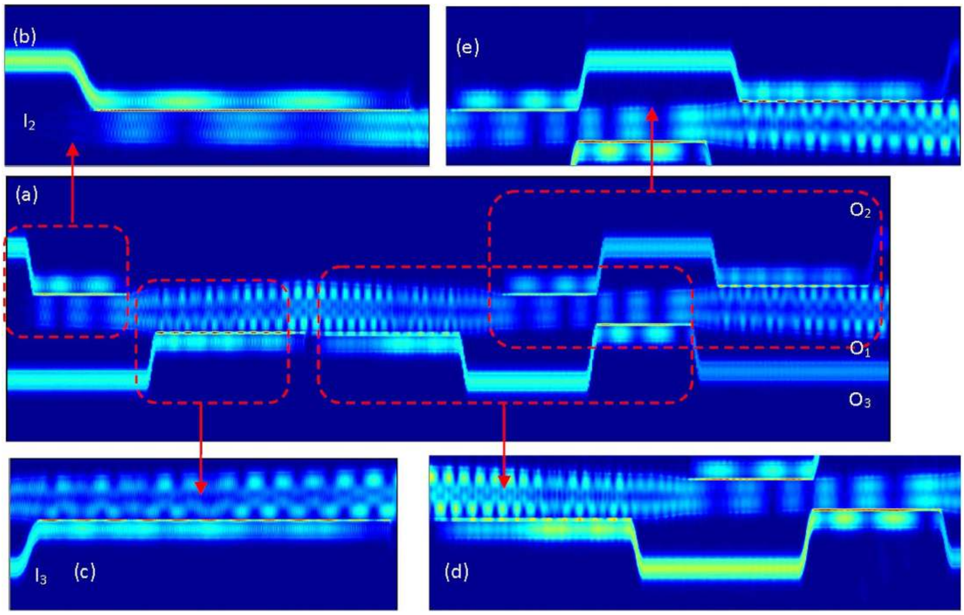

Figure 5. 3D FDTD simulation results of light propagation for optical mode multiplexing and mode exchange.

TE_0 mode propagates directly in the multimode bus waveguide. Figure 6(b–h) show the case when only I_2 port is launched by TE_0 mode. The whole mode evolution process from TE_0-TE_1-TE_0-TE_2 is depicted in Fig. 6(h), implying the mode conversion from TE_1 to TE_2 in the multimode bus waveguide. Shown in Fig. 6(f) is the zoomed in view of the TE_1 mode excitation by the input TE_0 mode. Figure 6(b,c) are the corresponding field profiles of TE_0 mode and TE_1 mode monitored in the waveguide cross section. Shown in Fig. 6(g) is the zoomed in view of back conversion from TE_1 mode to TE_0 mode and its further conversion to TE_2 mode. Figure 6(d,e) are the corresponding field profiles of TE_0 mode and TE_2 mode monitored in the waveguide cross section. Figure 6(i–o) show the case when only I_3 port is launched by TE_0 mode. The whole mode evolution process from TE_0-TE_2-TE_0-TE_1 is depicted in Fig. 6(i), implying the mode conversion from TE_2 to TE_1 in the multimode bus waveguide. Shown in Fig. 6(j) is the zoomed in view of the TE_2 mode excitation by the input TE_0 mode. Figure 6(l,m) are the corresponding field profiles of TE_0 mode and TE_2 mode monitored in the waveguide cross section. Shown in Fig. 6(k) is the zoomed in view of back conversion from TE_2 mode to TE_0 mode and its further conversion to TE_1 mode. Figure 6(n,o) are the corresponding field profiles of TE_0 mode and TE_1 mode monitored in the waveguide cross section. According to the mode conversion from TE_1 to TE_2 in the multimode bus waveguide shown in Fig. 6(b,h) and the mode conversion from TE_2 to TE_1 in the multimode bus waveguide shown in Fig. 6(I–o), one can expect the mode exchange between the TE_1 mode and TE_2 mode in the multimode bus waveguide.

Figure 7(a–c) show the normalized transmission responses at the three output ports O_1, O_2 and O_3, in which the light is launched into the input ports I_1, I_2 and I_3, respectively. Note that output ports O_1, O_2 and O_3 correspond to the total three modes (TE_0, TE_1, TE_2) after mode exchange between TE_1 and TE_2, the residual TE_0 mode during the TE_1-TE_0-TE_2 process (mode conversion from TE_1 to TE_2), and the residual TE_0 mode during the TE_2-TE_0-TE_1 process (mode conversion from TE_2 to TE_1), respectively. It can be seen that O_1 always has the maximum output response among the three output ports. The excess loss is less than 0.5 dB, showing efficient operation of mode exchange. Meanwhile, the extinction ratio defined by $10 \cdot \log_{10}(P_1 / P_i)$ (P_1 and P_i are normalized response at output port O_1 and O_i, $i = 2, 3$) is assessed to be larger than 15 dB within a 10 nm wavelength range from 1535 to 1545 nm. The obtained results shown in Figs 5–7 indicate favorable operation performance of efficient optical mode exchange, which might find interesting applications in robust on-chip network management by exploiting the spatial mode dimension.

Discussion

In summary, we have proposed on-chip optical mode exchange on SOI platform. The device is based on tapered directional couplers and has a relatively large fabrication error tolerance. The fabrication of the device could be easily realized by single step electron beam lithography followed by inductively coupled plasma etching. The obtained simulation results show effective mode excitation and efficient mode exchange between TE_1 and TE_2 modes. A low excess loss less than 0.5 dB and a high extinction ratio larger than 15 dB over a 10 nm wavelength range from 1535 to 1545 nm are achieved. With the obtained results, we believe that optical data exchange in the mode domain could be further realized when each

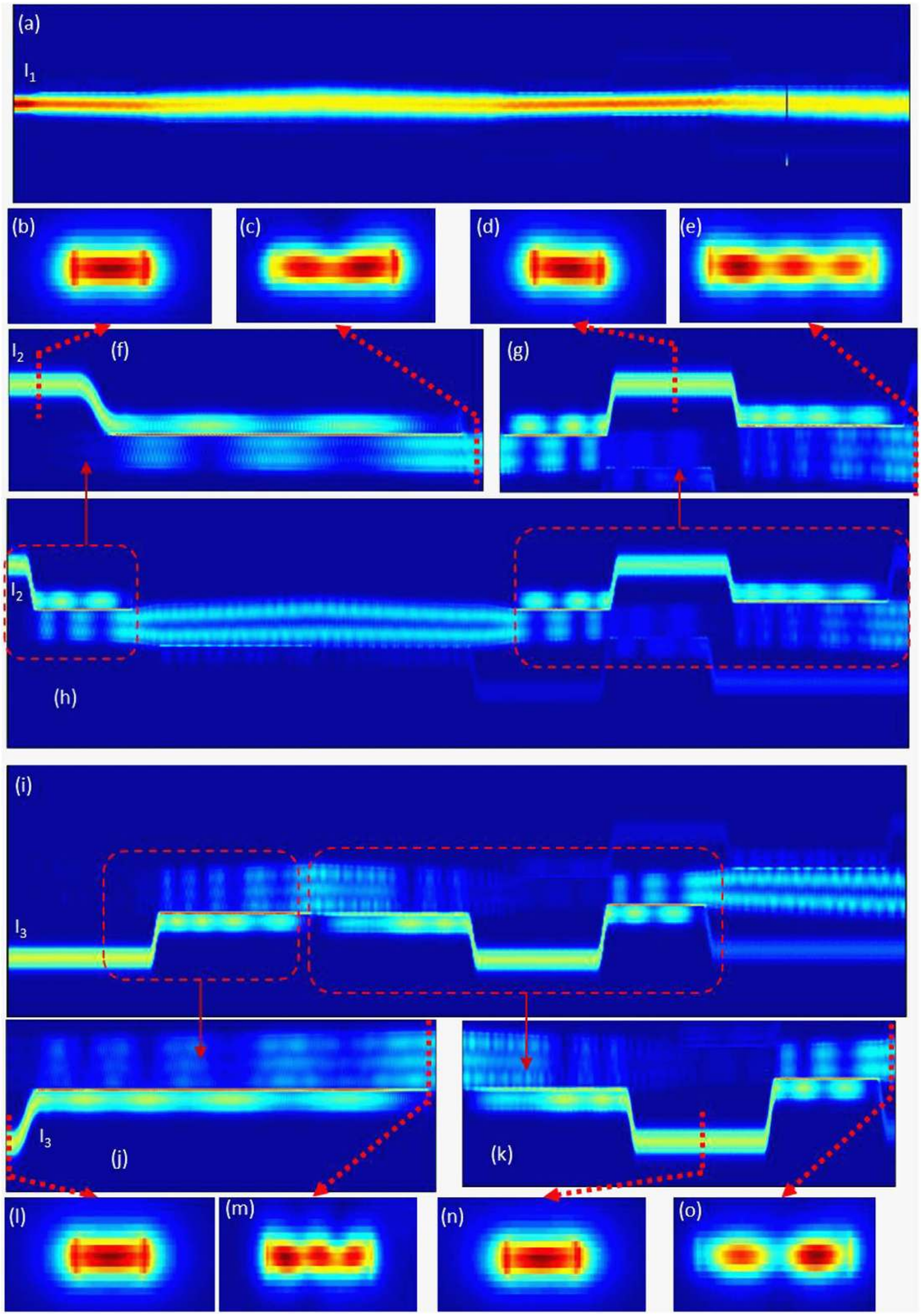

Figure 6. 3D FDTD simulation results of light propagation when only (**a**) I_1 port, (**b–h**) I_2 port, or (**i–o**) I_3 port is launched by TE_0 mode.

mode carries different data information. The proposed optical mode exchange might facilitate flexible optical data processing functions in an on-chip mode multiplexing systems.

Method

The mode properties (mode distribution and effective refractive index) of the guided modes in the silicon nanowire are calculated by using finite-element method (FEM) with COMSOL^{TM}. The scattering bound condition is considered and the simulation domain is surrounded by rectangular perfectly matched layer (PML). The light propagation is simulated by a three dimensional finite difference time domain (3D FDTD) method.

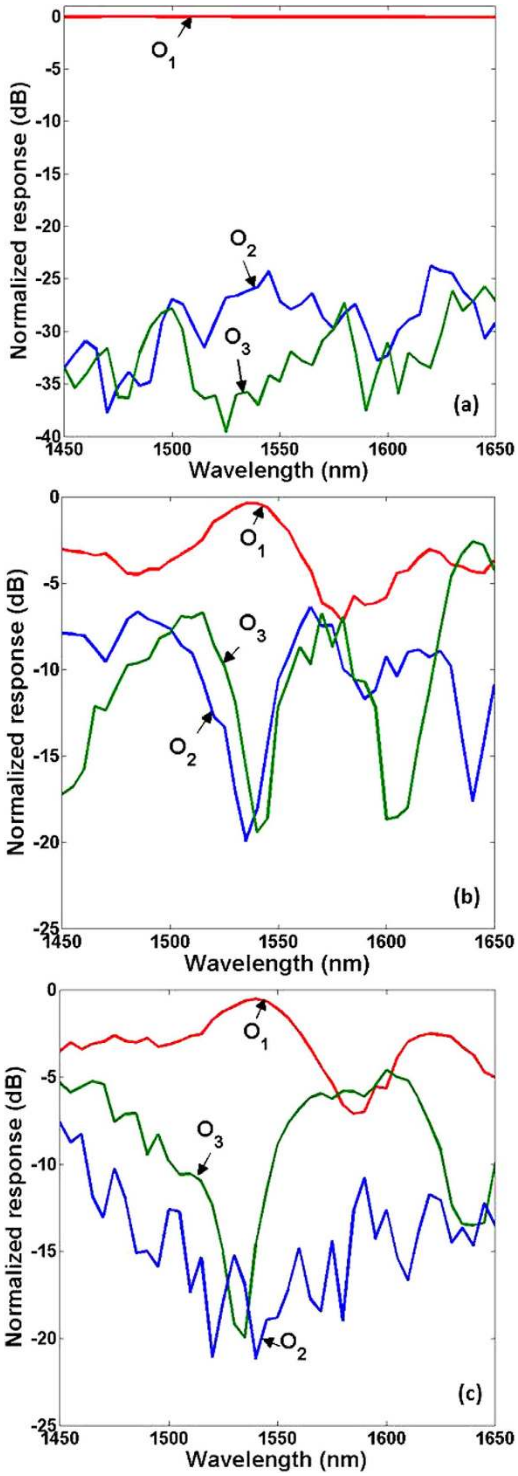

Figure 7. Normalized responses at output ports (O_1, O_2 and O_3) when light is launched into input port (**a**) I_1, (**b**) I_2 and (**c**) I_3.

References

1. Shacham, A. *et al.* Photonic networks-on-chip for future generations of chip multiprocessors. *IEEE Trans. Comput.* **57,** 1246–1260 (2008).
2. Doerr, C. & Taunay, T. Silicon photonics core-, wavelength-, and polarization-diversity receiver. *IEEE Photon. Technol. Lett*. **23,** 597–599 (2011).
3. Randel, S. *et al.* 6 × 56-Gb/s mode-division multiplexed transmission over 33-km few-mode fiber enabled by 6 × 6 MIMO equalization. *Opt. Express* **19,** 16697–16707 (2011) .
4. Veldhuis, G. J. *et al.* Design and characterization of a mode-splitting Ψ-junction. *J. Lightwave Technol.* **14,** 1746–1752 (1996).

5. Shirafuji, K. & Kurazono, S. Transmission characteristics of optical asymmetric Y junction with a gap region. *J. Lightwave Technol.* **9,** 426–429 (1991).
6. Love, J. D. & Riesen, N. Single-, few-, and multimode Y-junctions. *J. Lightwave Technol.* **30,** 304–309 (2012).
7. Riesen, N. & Love, J. D. Design of mode-sorting asymmetric Y-junctions. *Appl. Opt.* **51,** 2778–2783 (2012).
8. Kawaguchi, Y. & Tsutsumi, K. Mode multiplexing and demultiplexing devices using multimode interference couplers. *Electron. Lett.* **38,** 1701–1702 (2002).
9. Uematsu, T. *et al.* Design of a compact two-mode multi/demultiplexer consisting of multimode interference waveguides and a wavelength-insensitive phase shifter for mode-division multiplexing transmission. *J. Lightwave Technol.* **30,** 2421–2426 (2012).
10. Xing, J. *et al.* Two-mode multiplexer and demultiplexer based on adiabatic couplers. *Opt. Lett.* **38,** 3468–3470 (2013).
11. Dai, D. *et al.* Silicon mode (de)multiplexer enabling high capacity photonic networks-on-chip with a single-wavelength-carrier light. *Opt. Lett.* **38,** 1422–1424 (2013).
12. Wang, J. *et al.* On-chip silicon 8-channel hybrid (de)multiplexer enabling simultaneous mode- and polarization-division-multiplexing. *Laser Photon. Rev.* **8,** L18–L22 (2014).
13. Ding, Y. *et al.* On-chip two-mode division multiplexing using tapered directional coupler-based mode multiplexer and demultiplexer. *Opt. Express* **21,** 10376–10382 (2013).
14. Hamza, H. S. & Deogun, J. S. Wavelength-exchanging cross connects (WEX) - A new class of photonic cross-connect architectures. *J. Lightwave Technol.* **24,** 1101–1111 (2006).
15. Uesaka, K. *et al.* Wavelength exchange in a highly nonlinear dispersion-shifted fiber: theory and experiments. *IEEE J. Sel. Top. Quantum Electron.* **8,** 560–568 (2002).
16. Fung, R. W. L. *et al.* Widely tunable wavelength exchange in anomalous-dispersion regime. *IEEE Photon. Technol. Lett*. **19,** 1846–1848 (2007).
17. Shen, M. *et al.* Byte-level parametric wavelength exchange for narrow pulsewidth return-to-zero signal. *IEEE Photon. Technol. Lett.* **21,** 1591–1593 (2009).
18. Gao, Y. *et al.* Wavelength interchange of phase-shift-keying signal. *IEEE Photon. Technol. Lett.* **22,** 838–840 (2010).
19. Wang, J. *et al.* Reconfigurable 2.3-Tbit/s DQPSK simultaneous add/drop, data exchange and equalization using double-pass LCoS and bidirectional HNLF. *Opt. Express* **19,** 18246–18252 (2011).
20. Gui, C. C. & Wang, J. Optical data exchange of m-QAM signals using a silicon-organic hybrid slot waveguide: proposal and simulation. *Opt. Express* **22,** 24796–24807 (2014).
21. Zhang, Z., Gui, C. C. & Wang, J. On-chip optical mode multicasting using tapered directional coupler. In *Asia Communications and Photonics Conference* (ACP), Optical Society of America, paper ATh3A.53, 2014.

Acknowledgements

This work was supported by the National Natural Science Foundation of China (NSFC) under grant 61222502, the Program for New Century Excellent Talents in University (NCET-11-0182), the Wuhan Science and Technology Plan Project under grant 2014070404010201, the Fundamental Research Funds for the Central Universities (HUST) under grants 2012YQ008 and 2013ZZGH003, and the seed project of Wuhan National Laboratory for Optoelectronics (WNLO). The authors thank Chengcheng Gui for valuable technical supports and helpful discussions.

Author Contributions

J.W. developed the concept and conceived the design. Z.Z. and X.H. performed the numerical simulations. Z.Z. and J.W. analyzed the data. Z.Z., X.H. and J.W. contributed to writing and finalizing the paper. J.W. supervised the project.

Additional Information

Competing financial interests: The authors declare no competing financial interests.

How to cite this article: Zhang, Z. *et al.* On-chip optical mode exchange using tapered directional coupler. *Sci. Rep.* **5**, 16072; doi: 10.1038/srep16072 (2015).